REGULAR ARTICLE

Revisiting the anatomy of the central nervous system of a hemimetabolous model insect species: the pea aphid *Acyrthosiphon pisum*

**Martin Kollmann · Sebastian Minoli · Joël Bonhomme ·
Uwe Homberg · Joachim Schachtner · Denis Tagu ·
Sylvia Anton**

Abstract Aphids show a marked phenotypic plasticity, producing asexual or sexual and winged or wingless morphs depending on environmental conditions and season. We describe here the general structure of the brain of various morphs of the pea aphid *Acyrthosiphon pisum*. This is the first detailed anatomical study of the central nervous system of an aphid by immunocytochemistry (synapsin, serotonin, and several neuropeptides), ethyl-gallate staining, confocal laser scanning microscopy, and three-dimensional reconstructions. The study has revealed well-developed optic lobes composed of lamina, medulla, and lobula complex. Ocelli are only present in males and winged parthenogenetic females. The central complex is well-defined, with a central body divided into two parts, a protocerebral bridge, and affiliated lateral accessory lobes. The mushroom bodies are ill-defined, lacking calyces, and only being visualized by using an antiserum against the neuropeptide orcokinin. The antennal lobes contain poorly delineated glomeruli but can be clearly visualized by performing antennal backfills. On the basis of our detailed description of the brain of winged and wingless parthenogenetic *A. pisum* females, an anatomical map is now available that should improve our knowledge of the way that these structures are involved in the regulation of phenotypic plasticity.

M. Kollmann · U. Homberg · J. Schachtner
Department of Biology - Animal Physiology,
Philipps University Marburg,
35043 Marburg, Germany

S. Minoli · S. Anton (✉)
Centre de Recherches de Versailles, INRA, UMR 1272 PISC,
F-78000 Versailles, France
e-mail: sylvia.anton@versailles.inra.fr

J. Bonhomme · D. Tagu (✉)
Domaine de la Motte, INRA Rennes, UMR1099 BiO3P,
BP35327, 35653 Le Rheu, France
e-mail: denis.tagu@rennes.inra.fr

Present Address:
S. Minoli
Laboratory of Insect Physiology (74b), DBBE, C1428EHA,
University of Buenos Aires,
Buenos Aires, Argentina

Abbreviations

5HT	Serotonin
a	Anterior
AL	Antennal lobe
AN	Antennal nerve
Asn^{13}-OK	Asn^{13}-orcokinin
CB	Central body
CBL	Lower division of the central body
CBU	Upper division of the central body
CNS	Central nervous system
d	Dorsal
DL	Dorsal lobe
G	Glomerulus
GA	Glutaraldehyde
l	Lateral

La	Lamina
LAL	Lateral accessory lobe
LALcom	Lateral accessory lobe commissure
Lodm	Lobula dorso-median lobe
Loi	Lobula inner lobe
Loo	Lobula outer lobe
LoX	Lobula complex
Mas-AT	*Manduca sexta* allatotropin
MB	Mushroom body
Me	Medulla
MeD1 D2	Medulla divisions
mL	Mushroom body median lobe
NGS	Normal goat serum
OL	Optic lobe
PB	Protocerebral bridge
PBS	Phosphate-buffered saline
PFA	Paraformaldehyde
Pea-PVK-II	*Periplaneta americana* perivis013cerokinin II
RT	Room temperature
SEG	Subesophageal ganglion
TGM	Thoracic ganglionic mass
TrX	Triton X
v	Ventral
vL	Mushroom body ventral lobe

Introduction

Aphids are insect pests that feed on plant phloem sap, a sugar-rich plant juice containing all nutritive elements required for their survival and reproduction. Despite this highly restrictive life style, aphids live at a nexus of abiotic and biotic interactions (for a review, see Tagu et al. 2008), such as changes of host plants, natural enemies, and local environments. This implies, as for many animals, the necessity to detect visual, tactile, chemical, and other sensory signals. Aphids are able to adapt their behavior to the environmental situation through neuro-endocrine regulation of their sensory systems and cellular responses (Le Trionnaire et al. 2008).

Aphids have the peculiarity of propagating through viviparous parthenogenesis. The genome functioning of aphids is highly plastic, since a given genotype can produce alternative phenotypes such as winged or wingless, parthenogenetic or sexual, and in some cases, soldier morphs (Simon et al. 2010). The development of the different morphs depends on local environmental cues sensed by the adult parthenogenetic mothers. Crowding triggers the birth of soldiers or winged individuals that will escape the unfavorable environment and explore new plants (for a review, see Simon et al. 2010). Photoperiod shortening in autumn triggers the switch from parthenogenetic to sexual

reproduction, in which fertilized oviparous sexual females lay overwintering eggs (for a review, see Le Trionnaire et al. 2008). This high level of phenotypic plasticity is unique and not only implies the necessity for the aphid to detect and process certain environmental cues, but also the enormous plasticity of its sensory and central nervous system (CNS).

The CNS of hemipteran insects is characterized by highly fused ganglia (Hanström 1928; Pflugfelder 1937). The antennal nerves enter the brain ventrally and branch in glomerular or aglomerular antennal lobes (ALs; Pflugfelder 1937). In several hemipteran species, the larval visual system persists through the adult stage, in addition to three optic ganglia only present in adults (Pflugfelder 1937). The mushroom bodies (MBs) might develop, depending on the lifestyle of the species, and calyces and vertical or medial lobes can be missing (Kenyon 1896; Kühnle 1913; Pflugfelder 1937). The protocerebral bridge (PB) and a central body (CB) consisting of two parts are generally well developed (Pflugfelder 1937). Within the hemiptera, the aphid brain has been thoroughly described by Pflugfelder (1937); some studies from the late 1960s and 1970s have added information (e.g. Lees 1964; Gabriel 1965; Steel 1977; Steel and Lees 1977), but only a few more recent accounts have been published (e.g., Hardie 1987a, 1987b; Tilley et al. 2000). The aphid brain is commonly divided into the protocerebrum, including the optic lobes (OLs), the central complex, the MBs, the deutocerebrum with the ALs and dorsal lobes (DLs), and the tritocerebrum, the most ventral part of the brain associated with the mouthparts (Hardie 1987a, 1987b). The subesophageal ganglion (SEG) is situated at the posterior end of the head capsule, and the thoracic ganglionic mass (TGM) results from the fusion of all thoracic and abdominal ganglia.

Because of its particular lifestyle and reproduction, the stomatogastric and neuroendocrine systems of aphids have received special attention. Various groups of neurosecretory cells in the protocerebrum have been distinguished based on paraldehyde-fuchsin staining (for a review, see Hardie 1987a). Axonal projections have been traced from the protocerebrum to the corpora cardiaca (a paired neurosecretory gland), the SEG, and the TGM. Some projections continue to the hindgut and, in some cases, might even reach the ovaries, although this observation has never verified since the study of Steel (1977). The chemical nature of neurosecretions is unknown, but local cauterization of protocerebral group I neurosecretory cells is responsible for the failure in autumn conditions to switch from parthenogenetic to sexual reproduction (Steel and Lees 1977). Concerning the endocrine system, the corpus allatum (producing the juvenile hormones) found in adult aphids originates from the fusion of the two corpora allata present in embryos or in larvae and is connected to the

corpora cardiaca. The prothoracic glands (producing ecdy-steroids) are connected to protocerebral group II secretory cells by axonal projections (Hardie 1987b).

The description of the aphid CNS has so far remained rudimentary, despite two major technological advances: the development of genomic resources and the tremendous improvement in imaging technology and immunocyto-chemical tools. Functional genomics has identified several genes that are regulated during photoperiod shortening, many of them being involved in neuro-endocrine signaling (e.g., insulin, dopamine; Le Trionnaire et al. 2007, 2009; Gallot et al. 2010). The genome annotation of *A. pisum* has allowed the identification of 42 neuropeptides and neuro-hormones (Huybrechts et al. 2010). These are promising candidates for playing key roles in regulating sensory detection and neuronal processing of biotic and abiotic signals in aphids. Today, advanced histological techniques and confocal laser scanning microscopy allow a more detailed description of the architecture of neural tissues and high-resolution analyses of neuropils. Such a detailed description not only enables us to identify target areas of neuromodulatory action, but also provides the basis for investigating anatomical differences between morphs of diverse life styles, requiring, for example, different degrees of integration of different sensory inputs. This work aims at revisiting the CNS morphology of winged and wingless parthenogenetic pea aphids in order to provide an anatomical base for future functional analyses in aphid neurobiology. We describe the main CNS features of *A. pisum* following classical overview staining with the osmium/ethyl-gallate technique, antennal back-fills, and immunocytochemical methods, followed by three-dimensional reconstructions.

Materials and methods

Insects

The genetic clone *Acyrthosiphon pisum* LSR1 genotype was reared on broad bean plants (*Vicia fabae*) at 18°C under a 16-h light:8-h dark photoperiod regime to maintain clonal reproduction of the colony. The production of winged parthenogenetic females was induced by retaining high densities of individuals on one plant.

Osmium/ethyl-gallate staining

Osmium/ethyl-gallate staining was carried out according to Leise and Mulloney (1986). Head capsules were cut open and immersed in 2% glutaraldehyde (GA) and 1% paraformaldehyde (PFA; Roth, Karlsruhe, Germany) in cacodylate buffer (Sigma-Aldrich, Saint-Quentin Fallavier,

France; 0.16 M, pH 7.2), containing 1.3 g sucrose/100 ml, overnight at room temperature (RT) on a rotator. Heads were briefly washed in cacodylate buffer and incubated overnight in 1% osmium tetroxide solution (Sigma-Aldrich) in distilled water in the dark at 4°C on a rotator. They were again washed (3×10 min) in cacodylate buffer at 4°C, transferred to a supersaturated ethyl gallate (Sigma-Aldrich) solution overnight at 4°C in the dark, washed (2×10 min) in cacodylate buffer, dehydrated in 5-min steps in an ascending ethanol series (50%, 70%, 96% and 100%), and transferred to propylene oxide. Whole heads were then placed in 1:1 propylene oxide:Durcupan (Fluka, Buchs, Switzerland) in open vials for 6-8 h, followed by 100% Durcupan for 5-8 h, embedded in fresh Durcupan in silicon capsules, and polymerized overnight at 60°C. Sections were cut at a thickness of 10 μm with a glass knife on a microtome (RM2055, Leica Jung, Rueil-Malmaison, France).

Antisera

For immunostaining, we used rabbit antisera against *Manduca sexta* allatotropin (Mas-AT), *Orconectes limosus* Asn[13]-orcokinin (Asn[13]-OK), *Periplaneta americana* peri-viscerokinin II (Pea-PVK-II), serotonin (5HT), the catalytic subunit of *Drosophila melanogaster* protein kinase A (DC 0), and a monoclonal antibody from mouse against the *D. melanogaster* synaptic vesicle protein synapsin I (SYN-ORF1). Recent annotation of the pea aphid genome suggested that many of the known insect neuropeptides had been detected in *A. pisum* (Huybrechts et al. 2010; accession number for orcokinin: ACYPIG995519, and for allatotropin: ACYPIG976664), a good indication that heterologous antibodies could be used with success to localize neuropeptides in the pea aphid CNS. The antiserum against Mas-AT was used at a concentration of 1:4000 (no. 13.3.91, kindly provided by Dr. J. Veenstra, University of Bordeaux, Talence, France; Veenstra and Hagedorn 1993). Specificity had previously been tested by enzyme-linked immunosorbent assay in the sphinx moth *Manduca sexta* and the cockroach *Periplaneta americana* by Veenstra and Hagedorn (1993). The antiserum recognizes Mas-AT (Kataoka et al. 1989) and *Locusta* myo-tropin (Veenstra and Hagedorn 1993), both ending with TARGFamide. The Asn[13]-OK antiserum (generously provided by Dr. H. Dircksen, University of Stockholm, Sweden) was used at a concentration of 1:1000. The antiserum was produced by GA coupling of synthetic Asn[13]-orcokinin (NFDEIDRSGFGFN) of the crayfish *O. limosus* to bovine thyroglobulin (Bungart et al. 1994). Specificity tests were performed for nervous tissue of various astacidean crustaceans (Bungart et al. 1994), the cockroach *Leucophaea maderae*, the locust *Schistocerca*

gregaria, and the silverfish *Lepisma saccharina* (Hofer et al. 2005). The antiserum against Pea-PVK-II (kindly provided by Dr. M. Eckert, University of Jena, Germany; Eckert et al. 2002) was used at a concentration of 1:2500. The antiserum was raised against Pea-PVK-II (GSSGLISMPRVa) of *P. americana*; it recognizes peptides C-terminally ending with PRXamide (Eckert et al. 2002). Preadsorption of the diluted antiserum with 50 μg and 100 μg of the peptide abolished all immunostaining in brains of *P. americana* (Eckert et al. 2002). A polyclonal serotonin (5HT) antibody produced in rabbit (Sigma S5545) was used at a concentration of 1:200 (Huang et al. 2005). The DC 0 antibody recognizes the catalytic subunit of protein kinase A of *D. melanogaster* (1:500; kindly provided by Dr. D. Kalderon, Columbia University, N.Y., USA; Lane and Kalderon 1993). It labels the Kenyon cells in the MBs of all neopteran insects studied so far (Farris and Sinakevitch 2003; Farris and Strausfeld 2003; Farris et al. 2004; Farris 2005). The specificity of the antiserum has been demonstrated in the honeybee *Apis mellifera* and the fruit fly *D. melanogaster* (Fiala et al. 1999).

The monoclonal antibody from mouse against a fusion protein, consisting of glutathione-S-transferase and the first amino acids of the presynaptic vesicle protein synapsin I coded by its 5′-end, from *D. melanogaster* (SYNORF1; Klagges et al. 1996), was used selectively to label neuropil areas in the brain (3 C11, no. 151101 [13.12.06])). It was kindly provided by Dr. E. Buchner (University of Würzburg, Germany) and used at a concentration of 1:50. Specificity had been tested in *M. sexta*, the red flour beetle *Tribolium castaneum*, and *D. melanogaster* (Utz et al. 2008).

Immunocytochemistry

Brains were dissected in cold Millonig's buffer (83.9 ml 0.164 M $NaH_2PO_4.H_2O$, 16.1 ml 0.63 M NaOH, 1.3 g sucrose, pH 7.2) and immediately fixed in 4% PFA (Roth) in buffer overnight at 4°C. Brains were then rinsed (4×10 min) at RT in buffer followed by preincubation overnight at 4°C in 4% normal goat serum (NGS; Jackson Immuno-Research, Westgrove, Pa., USA) in buffer containing 4% Triton X-100 (TrX; Sigma-Albrich, Steinheim, Germany). We subsequently incubated the brains with the primary antibodies diluted in buffer containing 3% NGS and 0.25% TrX at 4°C for 3-5 days. We always combined the synapsin antibody from mouse with one of the rabbit antisera. The brains were then washed (4×10 min) in buffer containing 0.25% TrX and incubated for 3-4 days with secondary goat anti-mouse antibody conjugated to Cy5 and with goat anti-rabbit antibody conjugated to Cy3 (both 1/300, Jackson ImmunoResearch) diluted in buffer containing 1% NGS and 0.25% TrX. For the DC 0 antiserum, we alternatively used a goat anti-rabbit antibody conjugated to Alexa 488 (1:100; Molecular Probes, Invitrogen, Cergy Pointoise, France). After final washes in buffer (4×10 min), the brains were mounted in Vectashield (Vector laboratories, ABCYS, France) or 80% glycerol (Sigma-Aldrich) in buffer.

Autofluorescence

Brains were dissected in phosphate-buffered saline (PBS; 0.01 M phosphate, 0.1 M NaCl, pH 7.4) and fixed in 2% PFA and 2% GA in PBS for 3 or 4 days at 4°C. After being washed in PBS (4×15 min), brains were mounted in Vectashield.

Antennal backfills

Insects were immobilized by using double-sided tape on a slide, leaving the antennae free. One antenna was cut at the middle of the pedicel, and the stump was inserted into a glass capillary containing 1% Neurobiotin (Vector Laboratories, Burlingame, Calif., USA) in 0.25 M KCl. Animals were then maintained overnight at 4°C in a wet chamber. Dissections were subsequently performed in Millonig's buffer. Brains were immediately fixed overnight at 4°C in 4% PFA in Millonig's buffer, washed in Millonig's buffer (4×10 min), and preincubated overnight at 4°C with 4% TrX in Millonig's buffer. Neurobiotin was then visualized by incubation in 2.5% Oregon Green-avidin (Oregon Green 488 conjugate; Molecular Probes, Invitrogen), with 0.25% TrX and 3% NGS in Millonig's buffer for 3 days at 4°C. After being washed (4×10 min) in Millonig's buffer, brains were mounted in Vectashield.

Data analysis and three-dimensional reconstruction

Whole-mount fluorescent preparations were scanned with a confocal laser scanning microscope (Leica TCS SPE, Leica Microsystems Heidelberg, Germany) at 1024×1024 pixel resolution by using a 40× oil immersion objective (HCX PL FL 40×/0.75 0.17/D 0.40) or a 63× oil immersion objective (HCX PL APO 63×/1.40-0.60, Oil 0.17/E). All brains were scanned with a scanning speed of 400 or 200 Hz, a pinhole of 1 Airy unit, a step size of 1.0–0.4 μm, and a line average of 2-4. Images were cropped and arranged by using Adobe Photoshop CS2 (Adobe Systems, San Jose, Calif., USA) and CorelDRAW X3 (Corel, Ottawa, Ontario, CA); the contrast and brightness of Fig. 1e, f were optimized in Adobe Photoshop CS2.

Osmium/ethyl-gallate-stained sections were photographed with an Olympus BX50 microscope equipped with a 40× UPlanFl objective and a Camedia C2000Z camera with 2.1 Megapixel resolution (Olympus, Rungis, France).

Fig. 1 Central nervous system (CNS) and salivary gland of the aphid *Acyrthosiphon pisum* (*orientation bars*: *a* anterior, *d* dorsal, *v* ventral). **a, b** Three-dimensional projections of the CNS of a winged parthenogenetic animal, based on direct volume rendering of a synapsin-immunostained preparation, including the brain, the subesophageal ganglion (*SEG*), and the thoracic ganglionic mass (*TGM*). Note the circumesophageal connective (*arrow*) and the neck connective (*arrowhead*). **c** Stack of optical sections (maximum intensity projection) of the CNS and the salivary glands of a wingless parthenogenetic animal based on autofluorescence images. **d** Anterior view of a representation of the brain and selected neuropils (*AL* antennal lobe, *CB* central body, *DL* dorsal lobe, *La* lamina, *LAL* lateral accessory lobe, *LoX* lobula complex, *Me* medulla, *MB* mushroom body, *PB* protocerebral bridge). **e, f** Osmium/ethyl-gallate-stained sections through the head capsule of a wingless parthenogenetic female from anterior (**e**) to posterior (**f**). *Bars* 100 μm
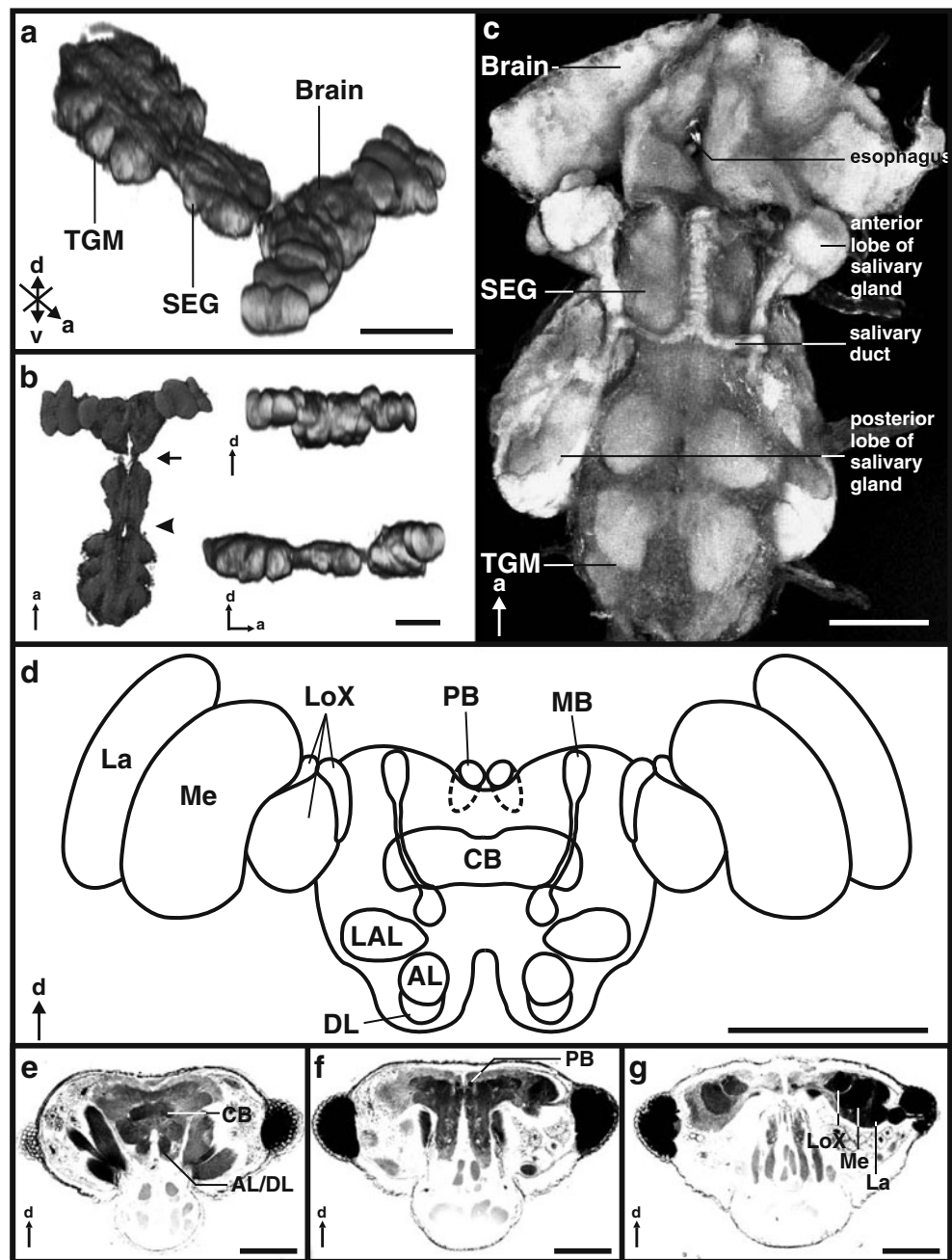
For three-dimensional reconstructions brain structures were labeled by using the segmentation editor and were reconstructed by using the polygonal surface model in AMIRA 4.1 or 5.1 (Visage Imaging, Fürth, Germany). Segmentation and reconstruction were performed according to previously published procedures (Kurylas et al. 2008). Standard color codes were used for the reconstructed neuropils (Brandt et al. 2005). For the visualization of the CNS including the brain, SEG, and TGM, we used direct volume rendering. For a comparison of neuropil volume, we compared the CB volume of 16 winged and 13 wingless

females and the AL volume of 6 winged and 10 wingless females, measured in synapsin-immunostained brains with the MaterialStatistics tool of AMIRA. The size of brains was determined by measuring the width of the protocerebrum (from left to right lamina) in frontal sections at the level of the center of the CB of 12 winged and 21 wingless females, based on osmium/ethyl-gallate staining. For statistical analyses, we used ANOVA tests (Sokal and Rohlf 1995) in SPSS (SPSS, IBM, Chicago, Ill., USA).

The representation of the brain in Fig. 1c was created in CorelDRAW X3 based on osmium/ethyl-gallate stain-

ing and synapsin immunostaining. The images of the immunostaining and of the reconstructions were imported from AMIRA into CorelDRAW X3 without further modification.

Results

General organization of the nervous system

Three-dimensional imaging of the nervous system from confocal sections provided a global overview of the CNS of the pea aphid (Fig. 1a, b). The main parts of the CNS were clearly identified, including the brain, the SEG, and the TGM containing the fused pro-, meso-, and metathoracic ganglia.

Whereas the brain and SEG are situated inside the head capsule, the TGM is situated partly inside the head and partly in the prothorax. When dissecting the CNS of the pea aphid, the salivary glands remain attached to it. They consist of two large cylindrical structures placed either side of the TGM. They connect anteriorly to the secondary salivary glands, which are smaller and lie beside the SEG (Fig. 1c). The ducts of the four glands fuse medially, ventral to the esophagus, at the level of the neck connectives (Fig. 1c). The esophagus then advances anteriorly over the SEG, turning ventrally to enter the stylets.

The SEG in *A. pisum* is anteriorly connected to the tritocerebrum via the circumesophageal connectives (Fig. 1b, arrow) and posteriorly to the thoracic ganglia via the neck connectives (Fig. 1b, arrowhead). The TGM is composed of three paired ill-defined subunits corresponding to the pro-, meso-, and metathoracic ganglia. The CNS measured on average 630 μm (SE=6.3 μm; $n=6$) from the anterior end of the brain to the posterior end of the TGM.

The brain is classically structured, with a dorsally situated protocerebrum (OLs, MBs, central complex, including CB and PB, and lateral accessory lobes [LALs]), medially situated deutocerebrum (AL and DL, the latter equivalent to the antennal mechanosensory and motor center), and ventrally situated tritocerebrum (Fig. 1d-f). The maximum width of the brain measured at the level of the OLs was on average 380 μm (SE=10.6 μm; $n=21$). The size of the brain was not significantly different ($P=0.84$) between winged ($n=12$) and wingless ($n=21$) parthenogenetic females.

Protocerebrum

The protocerebrum consists of the paired hemispheres of the central brain and the two OLs. The central complex occupies the central part of the protocerebrum and is situated posterior-medially to the LALs. The MBs are difficult to identify with the methods that we have used (see

below), in contrast to the well-developed PB, which is prominent within the posterior part of the protocerebrum (Fig. 1d-f).

The OLs (Figs. 1d, g, 2), attached to the retina, are subdivided into a well-developed lamina (La), medulla (Me), and lobula complex (LoX; Figs. 1d, 2). The LoX consists of three subunits, an inner lobe (Loi), an outer lobe (Loo), and a dorso-median lobe (Lodm; Fig. 2a-c, k). The Me is organized into two divisions. An outer and an inner Me could be distinguished following synapsin immunostaining (Fig. 2d; MeD1 and MeD2). By using additional antibodies, we stained immunoreactive layers that could not be identified by the anti-synapsin staining alone: anti-Pea-PVK-II (Fig. 2e, arrowheads), anti-Mas-AT (Fig. 2f, arrowheads), and anti-5HT (Fig. 2g, arrowheads). However, we could not determine the exact number of these layers.

Ocelli are present only in winged parthenogenetic females and in apterous males but are absent in apterous parthenogenetic and sexual females: a pair of lateral ocelli located antero-dorsally from the compound eyes is connected medially with the protocerebral lobes. The third ocellus lies medially between the bases of the antenna (data not shown). The three ocellar cup neuropils have a similar hemispherical shape and a diameter of 40-50 μm (Fig. 2h-j). Synapsin immunostaining visualized photoreceptor cells within the ocellar neuropils (Fig. 2h-j).

The well-defined CB (Fig. 1e) is divided into an upper (CBU) and a lower (CBL) division (Fig. 1d, 3). The border between the two divisions is formed by a layer exhibiting intense synapsin immunoreactivity (Fig. 3e, arrows). Serotonin-immunoreactive neurons densely innervate the CBU with varicose processes (Fig. 3f). The width of the CB measured 75-85 μm. The CB in winged parthenogenetic females had a significantly larger volume (43607 μm³; SE=606 μm³; $n=16$) than the CB in wingless parthenogenetic females (37329 μm³; SE=685 μm³; $n=13$; $P=2.2\times10^{-7}$).

Following synapsin immunostaining, the PB appears as two bar-shaped hemispheres, arranged in a V-shaped form that opens posteriorly (Figs. 1d, 3g, h). The two PB hemispheres approach each other anteriorly but are not continuous across the brain midline (Fig. 3d). The LALs are well-defined by immunostaining for Asn[13]-OK (Fig. 3a) and 5HT (Fig. 4a). Both LALs are connected by a massive LAL commissure (LALcom; Figs. 3a, 4a).

The MBs are less well defined in the brain of *A. pisum* than in most other insects (for a review, see Strausfeld et al. 2009). We were, however, able to identify at least parts of the MBs through Asn[13]-OK immunostaining. Asn[13]-OK immunoreactivity was highly concentrated in the lobes, probably corresponding to the medial (Fig. 3a, b, mL) and vertical (Fig. 3a, b, vL) lobes of other insects. Pedunculi and calyces could not be identified. Up to four cell bodies
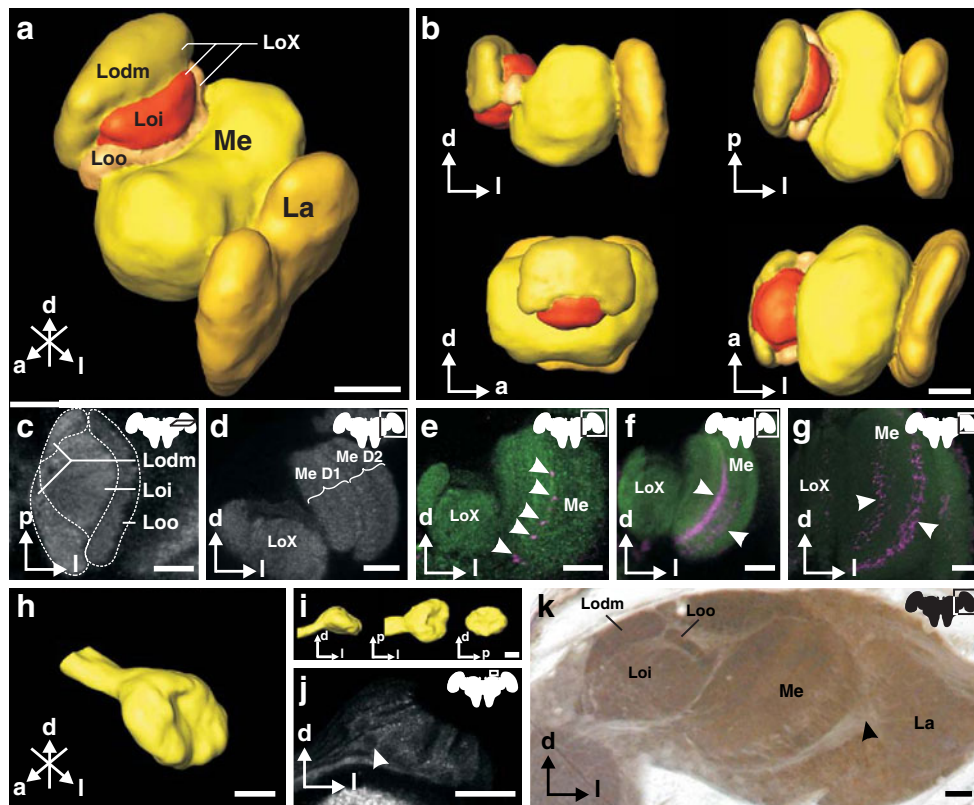
Fig. 2 Optic lobes (OLs) of the aphid *A. pisum* (*orientation bars*: *a* anterior, *d* dorsal, *l* lateral, *p* posterior). **a, b** Three-dimensional reconstruction of an OL of a winged parthenogenetic animal, based on synapsin immunostaining, showing the lamina (*La*), medulla (*Me*), and lobula complex (*LoX*). The LoX consists of three subunits, an inner lobe (*Loi*), an outer lobe (*Loo*), and a dorso-median lobe (*Lodm*). **c** Single optical section showing synapsin immunostaining of a winged parthenogenetic female. The inner, outer, and dorso-median lobes can be distinguished within the LoX (equivalent figure but without dashed lines is available in Electronic Supplementary Material Fig. S1a). **d** Synapsin staining of a wingless parthenogenetic animal showing the bipartition of the Me into two divisions (*Me D1*, *Me D2*). **e-g** Immunostaining with antisera against *Periplaneta americana* perivisccerokinin II (**e** wingless parthenogenetic animal), *Manduca sexta* allatotropin (**f** wingless parthenogenetic animal), and serotonin (**g** winged parthenogenetic animal) revealed layers (*magenta*, *arrowheads*) in the Me (*green* synapsin immunostaining). **h, i** Three-dimensional reconstructions of an ocellar nerve and neuropil of a winged parthenogenetic animal, based on synapsin immunostaining in **j**. **j** Synapsin immunostaining visualizes photoreceptor cells within the ocellus (*arrowhead*). **k** Osmium/ethyl-gallate-stained section through the optic lobe of a winged parthenogenetic animal. Note the optic chiasma between the La and Me (*arrowhead*) and the tripartite LoX. **c–g**, **j**, **k** *Insets top right* Position of the depicted brain areas. *Bars* 20 μm

per hemisphere were labeled with the DC 0 antibody at the dorsal border of the brain. Neurites extended toward the CB (Electronic Supplementary Material Fig. S1e), but whether these neurites belonged to Kenyon cells remained unclear.

Deutocerebrum

The ALs of *A. pisum* are located ventrally and medially near the esophagus (Figs. 1d, e, 4). They are relatively small spherical structures, measuring between 35 μm and 45 μm in diameter. The prominent antennal nerves (AN) enter the ALs ventro-laterally (Fig. 4c, d). Neurobiotin backfills of the antenna revealed fiber endings in the AL. Other fibers bypassed the AL, innervated the DL (Fig. 4d, e), and descended to the SEG (Fig. 4b, d, e, arrows). Glomerular structures within the AL could be identified in Neurobiotin-stained preparations (Fig. 4f). Each AL consisted of about 25-40 glomeruli. Delimitation of glomeruli was, however, difficult in most preparations, and a three-dimensional reconstruction of AL glomeruli was therefore not possible. Since glomeruli were not well separated from each other, no obvious difference in AL substructure was found between morphs. In one AL, spiny branches in a single glomerulus with a fiber projecting to the protocerebrum could be seen, probably representing a projection neuron (Fig. 4b, c, star). Because of obvious trans-synaptic staining, we could not tell whether descending fibers were part of primary afferents, or if they were higher order neurons. The AL exhibited strong 5HT immunoreactivity with sparse arborizations within the AL and varicose terminals. Each AL showed one fiber projecting dorsally toward unidentified medio-dorsal brain areas (Fig. 4a,
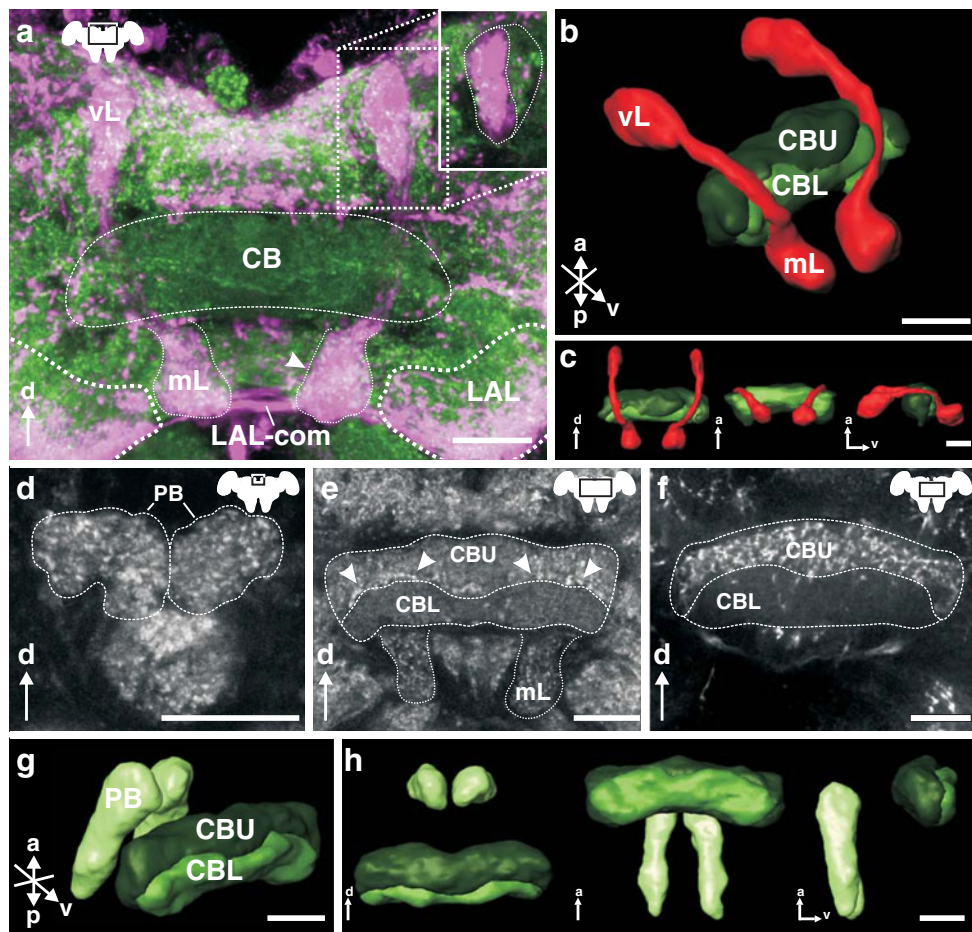
Fig. 3 Mushroom body (MB) and central complex of the aphid *Acyrthosiphon pisum* (orientation bars: *a* anterior, *d* dorsal, *p* posterior, *v* ventral). **a** Stack of optical sections (maximum intensity projection) showing synapsin (*green*) and Asn[13]-orcokinin (Asn[13]-OK, *magenta*) double-immunostaining in the median protocerebrum of a winged parthenogenetic animal with MB, central body (*CB*), and lateral accessory lobes (*LAL*) connected by a commissure (*LAL-com*). Strong Asn[13]-OK immunostaining is concentrated in the vertical lobe (*vL*) and medial lobe (*mL*) of the MB. *Inset top right* Optical section. Not all parts of the vertical lobes are Asn[13]-OK-immunoreactive. *Inset top left* position of the depicted brain area. **b, c** Three-dimensional reconstructions of the MBs and CB (*CBU* upper CB division, *CBL* lower CB division), based on synapsin and Asn[13]-OK immunostaining from preparation in **a**, including the vertical lobe (*vL*) and medial lobe (*mL*). **d** Optical section of a synapsin-immunostained brain of a winged parthenogenetic animal, showing the most anterior part of the protocerebral bridge (*PB*). Both arms of the PB touch each other at the midline of the brain (equivalent figure without dashed lines is available in Electronic Supplementary Material Fig. S1b). **e** Synapsin immunostaining of a wingless parthenogenetic animal, showing the upper and lower division of the central body (*CBU, CBL*). The border between the two divisions is marked by a layer of highly synapsin-immunoreactive fibers (*arrowheads*; equivalent figure without dashed lines is available in Electronic Supplementary Material Fig. S1c). **f** Differences in serotonin-immunoreactive profiles between the CBU and CBL of a winged parthenogenetic animal. Whereas the upper division shows strong serotonin immunostaining, the lower division is almost devoid of immunoreactive fibers (equivalent figure without dashed lines is available in Electronic Supplementary Material Fig. S1d). **d–f** *Insets top right* Position of the depicted brain areas. **g, h** Three-dimensional reconstructions of the central complex of a wingless parthenogenetic animal based on anti-synapsin staining. The two arms of the PB approach each other anteriorly. *Bars* 20 μm

arrows). The AL volumes of winged parthenogenetic females (40135 μm³; SE=1855 μm³; *n*=6) and of wingless parthenogenetic females (36910 μm³, SE=614 μm³; *n*=10) showed no significant difference (*P*=0.07).

The DL is a paired neuropil located ventral to the AL. The DL is not well delineated and could only be identified through backfills of probably non-olfactory afferents from the antenna (Fig. 4d, e).

Discussion

Organization of the aphid CNS

We have analyzed the organization of the CNS of the pea aphid *A. pisum* with emphasis on the brain. Although the general structure of the CNS in the pea aphid resembles the organization of the nervous system in other hemimetabolous
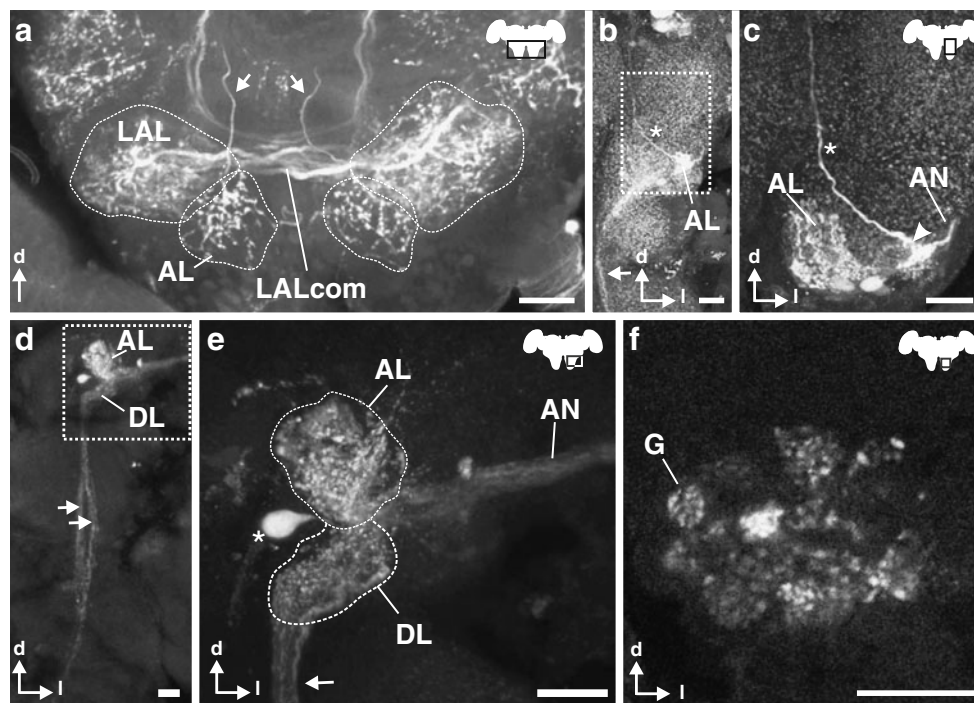
Fig. 4 Antennal lobes (*AL*) of the aphid *Acyrthosiphon pisum* (*orientation bars*: *d*dorsal, *l*lateral). **a-e** Stacks of optical sections (maximum intensity projection) of AL sections of wingless partheno-genetic females. **a** The ALs and the lateral accessory lobes (*LAL*), connected by the LAL commissure (*LALcom*) show strong serotonin (5HT) immunoreactivity. From each AL, a single 5HT-immunoreactive fiber (*arrows*) projects dorsally to an unidentified medio-dorsal brain area. **b** Backfills from the antenna typically resulted in staining of the antennal nerve (*AN*), the AL, and two additional fibers. **c** higher magnification of the *boxed area* in **b**. One of the fibers projected dorsally (*star*) into the protocerebrum. Because of the loss of staining intensity, this fiber could not be traced to its target area. The other fiber projected ventrally (*arrowhead*) toward the SEG. **d** The antenna backfill also showed that the AN entered both the AL and the dorsal lobe (*DL*). From the DL, two parallel fiber bundles projected ventrally into the SEG (*arrows*). **e** Higher magnification of the *boxed area* in **d**. In some samples, we also stained several cell bodies (*star*) attached to the AL and DL. **f** Optical section through an AL of a wingless parthenogenetic animal. Some of the antenna backfills revealed glomeruli (*G*) within the AL. **a**, **c**, **e**, **f** *Insets top right* Position of the depicted brain areas. *Bars* 20 μm

insects, clear differences have been found in comparison with sister groups, such as land-living Hemiptera, which have more developed MBs and a clearer glomerular organization of the ALs (Pflugfelder 1937; Pathak 1972; Kristoffersen et al. 2008; Barrozo et al. 2009). The highly fused nervous system of the pea aphid and the well-developed PC and CB are, on the other hand, common features of hemipteran brains (Pflugfelder 1937; Pathak 1972).

The OLs of *A. pisum* are well developed and can be divided into the classically described structures: the La, Me, and LoX. Interestingly, we have been able to identify a dorso-median subunit of the LoX resembling a lobula plate (Fig. 2a-c, k, Lodm). In other hemipteran species, a division of the lobula (also named medulla interna) into two subunits has been observed (Pathak 1972). Whether the parts of the third optic neuropil are homologous to the lobula and lobula plate described in Trichoptera, Lepidop-tera, Diptera, and Coleoptera (Strausfeld 2005) remains unclear. In other aphid species (e.g., *Aphis neeris*), larval

eyes consist of a few ommatidia ventrally adjacent to the adult compound eyes; their associated central neuropil, anterior to the adult La and dorso-medial to the adult Me, survive to the adult stage (Pflugfelder 1937). However, we have not found any indication of larval eyes and larval optic neuropil in adult pea aphids.

The CB of the pea aphid can be divided into an upper and a lower division (Fig. 3b, c, e-h) typical for a wide range of insect species (for a review, see Homberg 2008). At the ventral border of the CBU, we have identified a highly synapsin-immunreactive thin layer (Fig. 3e, arrows), forming a boundary to the CBL. With the exception of this highly synapsin-immunreactive layer, we have found no evidence for further layers within the CBU, as described in other insects (e.g., *S. gregaria*; Homberg 1991; *D. melanogaster*; Hanesch et al. 1989). The CBU, but not the CBL, contains serotonin-immunoreactive profiles (Fig. 3f) in accordance with findings in other insects (e.g., *S. gregaria*; Homberg 1991). Noduli, which are part of the central complex in other insect species (e.g., *D. mela-*

nogaster; Hanesch et al. 1989; *T. castaneum*; Dreyer et al. 2010), have not been identified with the staining methods used in the present study.

The PB of the pea aphid is folded and forms a huge V-shaped structure, opening posteriorly (Fig. 3g, h). At the anterior end of the V-shaped PB, the two branches are connected through a small fiber fascicle (Fig. 3d). This symmetric structure, connected via a small fiber bundle, is similar, although larger, than is common in other insects (for a review, see Homberg 2008).

The paired LALs, attached ventrolaterally to the CB, are interconnected by a commissure (LALcom). We have only been able to identify them by using Asn[13]-OK and 5HT antibodies (Figs. 3a, 4a). Their shape and position are, however, similar to those found in other insects (Pflugfelder 1937; Homberg 2008).

The MBs of *A. pisum* are highly reduced compared with those of other Pterygota and have only been identified by using the Asn[13]-OK antibody (Fig. 3a). We have only been able to identify structures that we interpret as a thin vertical lobe (Fig. 3a-c, vL) and a medial lobe (Fig. 3a-c, mL). Asn[13]-OK immunoreactivity of the MBs is known from several other insects and has been demonstrated in the medial and vertical lobes in *S. gregaria*, *L. maderae*, and *L. saccharina* (Hofer et al. 2005). The DC 0 antibody is well known for its ability to stain MBs in a variety of insects (for a review, see Strausfeld et al. 2009). The four DC 0-immunoreactive cell bodies in each hemisphere at the dorsal border of the brain (Electronic Supplementary Material, Fig. S1) might be related to a hypothetical calyx. However, synapsin or Asn[13]-OK antibodies do not label a structure resembling a calyx. We cannot exclude that the missing parts of the MB (calyx and pedunculus) have not been stained with the methods that we have used. Immunostaining with other antibodies need to be carried out in the future to determine whether parts of the MBs have indeed been "missed". FMRFamide immunoreactivity has been observed in these missing parts of the MB in many insects, such as *S. gregaria* (Homberg 2002), *M. sexta* (Homberg et al. 1990), or *A. mellifera* (Schürmann and Erbe, 1990). Moreover, a tachykinin-related peptide immunoreactivity of these missing MB parts are documented for several insects, such as *L. maderae* (Muren et al. 1995), the moth *Spodoptera litura* (Kim et al. 1998), or the locusts *Locusta migratoria* (Nässel 1993) and *S. gregaria* (Homberg 2002). However, our findings are consistent with previous studies describing aphid MBs as less developed and lacking calyces, compared with land-living Hemiptera (Kenyon 1896; Kühnle 1913; Hanström 1928; Pflugfelder 1937; for a review, see Strausfeld et al. 1998). MBs are generally considered as higher integration centers for olfactory and multimodal sensory input (for a review, see Strausfeld et al. 2009). They are often well developed in

insect species with complex social behavior and/or with a strong capacity for olfactory learning and memory (Hanström 1930; Heisenberg et al. 1985; Heisenberg 1998, 2003; Farris and Strausfeld 2003; Akalal et al. 2006). Anosmic insects, on the other hand, such as the Odonata and water-living beetles and bugs, show the same lack of MB calyces as aphids (Graichen 1936; Strausfeld et al. 1998), suggesting that olfactory cues play only a minor role in aphid behavior, in accordance with their rather sessile life style.

The ALs in *A. pisum* are connected to the antennae with long ANs and are situated in a ventral position; this might be attributable to the way that the antennae are inserted on the head. Although glomerular structures can be discerned in certain preparations by performing antennal backfills (Fig. 4f), glomeruli are not well delineated, as described in the aphid *Sitobion avenae* and in related hemipteran insect species (Kristoffersen et al. 2008; Barrozo et al. 2009). Possibly, glomeruli are not well separated by glial sheaths in aphids, as in Diptera (Stocker et al. 1990). Based on antennal backfills, we have, however, been able to obtain a rough estimate of 25-40 glomeruli for each AL of the pea aphid. A reduction of the AL in aphids toward an aglomerular structure might originate in the small number of olfactory receptor neurons present on the antenna. It coincides with only a minor role of olfaction in general in these insects, in accordance with the poorly developed higher olfactory integration centers, viz., the MBs, as mentioned above (Kristoffersen et al. 2008). In the pea aphid, however, 70 genes in the olfactory receptor family have been identified (The International Aphid Genomics Consortium 2010) and 15 genes coding for odorant-binding proteins (Zhou et al. 2010). Future functional studies are necessary to explain the discrepancy between the number of olfactory receptors and the number of glomeruli in the ALs and more generally to determine the importance of olfaction in these insects.

We have found ascending fibers from the AL into the protocerebrum (Fig. 4b, c, stars), but these neurons were only incompletely stained. These fibers might represent axons of projection neurons, projecting through an antenno-cerebral tract, as observed in other insect species (for a review, see Schachtner et al. 2005).

The ALs of *A. pisum* contain clear, but sparse, 5HT immunoreactivity concentrated in varicose terminals and a single fiber projecting toward the protocerebrum (Fig. 4a). We assume that each AL is innervated by one neuron, with a soma located medial to the AL. The position of the serotonin-immunoreactive soma and the ipsilaterally ascending projection to the protocerebrum correspond to that described in other Hemiptera (Dacks et al. 2006). The DLs, innervated by the ANs, are located ventral to the AL in the deutocerebrum (Fig. 4d, e) in a similar position to that in other insects (e.g., Pflugfelder

1937; Homberg et al. 1988; Staudacher et al. 2005; Barrozo et al. 2009).

Anatomical differences between morphs

No qualitative differences in brain anatomy have been found between the various morphs investigated, apart from the presence of ocelli, which exist only in winged parthenogenetic females and in apterous males, as described earlier (Anderson and Bromley 1987). The presence of ocelli has been classically associated with the capacity for fast signal transmission and horizon detection, which are important for fast flying insects (for a review, see Mizunami 1994). In *A. pisum*, not only winged females have ocelli, but also apterous males. The function of ocelli in these males is unknown but is probably related to visual cues essential for partner identification and localization.

The larger volume of the CB in winged parthenogenetic females than in wingless females might be attributable to differences in the mobility of the two morphs. Winged parthenogenetic females are morphs that develop to assure wider distribution. They are able to fly and need to orient with the help of sensory cues (probably primarily visual cues). The CB is generally thought to play an important role in spatial orientation and spatial and landmark-related visual memory (Strauss 2002; Homberg 2004, 2008). The CB might, thus, be more important in the more mobile winged aphid females than in sessile morphs.

Concluding remarks

We provide a precise anatomical description of the CNS of the pea aphid. With the help of this tool, we can now identify the specific areas involved in the switch between the different morphs of this species, by means of in situ hybridization and the immunocytochemical detection of neuropeptides that have been shown to be differentially expressed in the various morphs.

References

Akalal DBJ, Wilson CF, Zong L, Tanaka NK, Ito K, Davis RL (2006) Roles of *Drosophila* mushroom body neurons in olfactory learning and memory. Learn Mem 13:659–668

Anderson M, Bromley AK (1987) Sensory system. In: Minks AK, Harrewjin P (eds) Aphids, their biology, natural enemies and control, vol 1. Elsevier, Amsterdam, pp 153–162

Barrozo RB, Couton L, Lazzari CR, Insausti TC, Minoli SA, Fresquet N, Rospars JP, Anton S (2009) Antennal pathways in the central nervous system of a blood-sucking bug, *Rhodnius prolixus*. Arthropod Struct Dev 38:101–110

Brandt R, Rohlfing T, Rybak J, Krofczik S, Maye A, Westerhoff M, Hege HC, Menzel R (2005) Three-dimensional average-shape atlas of the honeybee brain and its applications. J Comp Neurol 492:1–19

Bungart D, Dircksen H, Keller R (1994) Quantitative determination and distribution of the myotropic neuropeptide orcokinin in the nervous system of astacidean crustaceans. Peptides 15:393–400

Dacks AM, Christensen TA, Hildebrand JG (2006) Phylogeny of a serotonin-immunoreactive neuron in the primary olfactory center of the insect brain. J Comp Neurol 498:727–746

Dreyer D, Vitt H, Dippel F, Goetz B, el Jundi B, Kollmann M, Huetteroth W, Schachtner J (2010) 3D standard brain of the red flour beetle *Tribolium castaneum*: a tool to study metamorphic development and adult plasticity. Front Systems Neurosci 4:3

Eckert M, Herbert Z, Pollak E, Molnar L, Predel R (2002) Identical cellular distribution of all abundant neuropeptides in the major abdominal neurohemal system of an insect (*Periplaneta americana*). J Comp Neurol 452:264–275

Farris SM (2005) Developmental organization of the mushroom bodies of *Thermobia domestica* (Zygentoma, Lepismatidae): insights into mushroom body evolution from a basal insect. Evol Dev 7:150–159

Farris SM, Sinakevitch I (2003) Development and evolution of the insect mushroom bodies: towards the understanding of conserved developmental mechanisms in a higher brain center. Arthropod Struct Dev 32:79–101

Farris SM, Strausfeld NJ (2003) A unique mushroom body substructure common to basal cockroaches and to termites. J Comp Neurol 456:305–320

Farris SM, Abrams AI, Strausfeld NJ (2004) Development and morphology of class II Kenyon cells in the mushroom bodies of the honey bee, *Apis mellifera*. J Comp Neurol 474:325–339

Fiala A, Müller U, Menzel R (1999) Reversible downregulation of protein kinase A during olfactory learning using antisense technique impairs long–term memory formation in the honeybee, *Apis mellifera*. J Neurosci 19:10125–10134

Gabriel CD (1965) Neurosekretion bei Aphiden. Wiss Z Univ Rostock 14:619–631

Gallot A, Rispe C, Leterme N, Gauthier JP, Jaubert-Possamai S, Tagu D (2010) Cuticular proteins and seasonal photoperiodism in aphids. Insect Biochem Mol Biol 40:235–240

Graichen E (1936) Das Zentralnervensystem von *Nepa cinerea* mit Einschluss des sympathischen Nervensystems. Zool Jahrb Abt Anat Ontog Tiere 61:195–238

Hanesch U, Fischbach KF, Heisenberg M (1989) Neuronal architecture of the central complex in *Drosophila melanogaster*. Cell Tissue Res 257:343–366

Hanström B (1928) Vergleichende Anatomie des Nervensystems der Wirbellosen Tiere. Springer, Berlin

Hanström B (1930) Über das Gehirn von *Termops nevadensis* und *Phyllium pulchrifolium* nebst Beitragen zur Phylogenie der Corpora pedunculata der Arthropoden. Z Morphol Oekol Tiere 19:732–773

Hardie J (1987a) Neurosecretory and endocrine systems. In: Minks AK, Harrewjin P (eds) Aphids, their biology, natural enemies and control, vol 1. Elsevier, Amsterdam, pp 139–152

Hardie J (1987b) Nervous system. In: Minks AK, Harrewjin P (eds) Aphids, their biology, natural enemies and control, vol 1. Elsevier, Amsterdam, pp 131–138

Heisenberg M (1998) What do the mushroom bodies do for the insect brain? An introduction. Learn Mem 5:1–10

Heisenberg M (2003) Mushroom body memoir: from maps to models. Nat Rev Neurosci 4:266–275

Heisenberg M, Borst A, Wagner S, Byers D (1985) *Drosophila* mushroom body mutants are deficient in olfactory learning. J Neurogenet 2:1–30

Hofer S, Dircksen H, Tollbäck P, Homberg U (2005) Novel insect orcokinins: characterization and neuronal distribution in the brains of selected dicondylian insects. J Comp Neurol 490:57–71

Homberg U (1991) Neuroarchitecture of the central complex in the brain of the locust *Schistocerca gregaria* and *S. americana* as revealed by serotonin immunocytochemistry. J Comp Neurol 2:245–254

Homberg U (2002) Neurotransmitters and neuropeptides in the brain of the locust. Microsc Res Tech 56:189–209

Homberg U (2004) In search of the sky compass in the insect brain. Naturwissenschaften 91:199–208

Homberg U (2008) Evolution of the central complex in the arthropod brain with respect to the visual system. Arthropod Struct Dev 37:347–362

Homberg U, Mantague RA, Hildebrand JG (1988) Anatomy of the antenno-cerebral pathways in the brain of the sphinx moth *Manduca sexta*. Cell Tissue Res 254:255–281

Homberg U, Kingan TG, Hildebrand JG (1990) Distribution of FMRFamide-like immunoreactivity in the brain and suboesophageal ganglion of the sphinx moth *Manduca sexta* and colocalization with SCP$_B$-, BPP-, and GABA-like immunoreactivity. Cell Tissue Res 259:401–419

Huang YJ, Maruyama Y, Lu KS, Pereira E, Plonsky I, Baur JE, Wu D, Roper SD (2005) Mouse taste buds use serotonin as a neurotransmitter. J Neurosci 25:843–847

Huybrechts J, Bonhomme J, Minoli S, Prunier-Leterme N, Dombrovsky A, Abdel-Latief M, Robichon A, Veenstra JA, Tagu D (2010) Neuropeptide and neurohormone precursors in the pea aphid, *Acyrthosiphon pisum*. Insect Mol Biol 19 (Suppl 2):87–95

The International Aphid Genomics Consortium (2010) Genome sequence of the pea aphid *Acyrthosiphon pisum*. PLoS Biol 8: e1000313. doi:10.1371/journal.pbio.1000313

Kataoka H, Toschi A, Li JP, Carney L, Schooley DA, Kramer SJ (1989) Identification of an allatotropin from adult *Manduca sexta*. Science 243:1481–1483

Kenyon CF (1896) The meaning and structure of the so-called mushroom bodies of the hexapod brain. Am Nat 30:643–650

Kim M-Y, Lee BH, Kwon D, Kang H, Nässel DR (1998) Distribution of tachykinin-related neuropeptide in the developing central nervous system of the moth *Spodoptera litura*. Cell Tissue Res 294:351–365

Klagges BRE, Heimbeck G, Godenschwege TA, Hofbauer A, Pflugfelder GO, Reifegerste R, Reisch D, Schaupp M, Buchner S, Buchner E (1996) Invertebrate synapsins: a single gene codes for several isoforms in *Drosophila*. J Neurosci 16:3154–3165

Kristoffersen L, Hansson BS, Anderbrant O, Larsson MC (2008) Aglomerular hemipteran antennal lobes—basic neuroanatomy of a small nose. Chem Senses 33:771–778

Kühnle K (1913) Vergleichende Untersuchungen über das Gehirn, die Kopfnerven, und Kopfdrüsen des gemeinen Ohrwurms (*Forficula auricularia*). Jena Z Naturwiss 50:147–276

Kurylas AE, Rohlfing T, Krofczik S, Jenett A, Homberg U (2008) Standardized atlas of the brain of the desert locust, *Schistocerca gregaria*. Cell Tissue Res 333:125–145

Lane ME, Kalderon D (1993) Genetic investigation of cAMP–dependent protein kinase function in *Drosophila* development. Genes Dev 7:1229–1243

Le Trionnaire G, Jaubert S, Sabater-Muñoz B, Benedetto A, Bonhomme J, Prunier-Leterme N, Martinez-Torres D, Simon JC, Tagu D (2007) Seasonal photoperiodism regulates the expression of cuticular and signalling protein genes in the pea aphid. Insect Biochem Mol Biol 37:1094–1102

Le Trionnaire G, Hardie J, Jaubert-Possamai S, Simon JC, Tagu D (2008) Shifting from clonal to sexual reproduction in aphids: physiological and developmental aspects. Biol Cell 100:441–451

Le Trionnaire G, Francis F, Jaubert-Possamai S, Bonhomme J, De Pauw E, Gauthier JP, Haubruge E, Legeai F, Leterme N, Simon JC, Tanguy S, Tagu D (2009) Transcriptomic and proteomic analyses of seasonal photoperiodism in the pea aphid. BMC Genomics 10:456

Lees AD (1964) The location of the photoperiodic receptors in the aphid *Megoura viciae* Buckton. J Exp Biol 41:119–133

Leise EMM, Mulloney B (1986) The osmium-ethyl gallate procedure is superior to silver impregnations for mapping neuronal pathways. Brain Res 367:265–272

Mizunami M (1994) Information processing in the insect ocellar system: comparative approaches to the evolution of visual processing and neural circuits. Adv Insect Physiol 25:151–265

Muren JE, Lundquist CT, Nässel D (1995) Abundant distribution of locustatachykinin-like peptide in the nervous system and intestine of the cockroach *Leucophaea maderae*. Philos Trans R Soc Lond Biol 348:423–444

Nässel DR (1993) Insect myotropic peptides: differential distribution of locustatachykinin- and leucokinin-like immunoreactive neurons in the locust brain. Cell Tissue Res 274:27–40

Pathak JPN (1972) Histology of the brain and optic lobes of *Halys dentata* F. (Hemiptera: Pentatomidae). Int J Insect Morphol Embryol 1:253–266

Pflugfelder O (1937) Vergleichend-anatomische experimentelle und embryologische Untersuchungen über das Nervensystem und die Sinnesorgane der Rhynchoten. Zoologica 34:1–102

Schachtner J, Schmidt M, Homberg U (2005) Organization and evolutionary trends of primary olfactory brain centers in Tetraconata (Crustacea+Hexapoda). Arthropod Struct Dev 34:257–299

Schürmann FW, Erber J (1990) FMRFamide-like immunoreactivity in the brain of the honeybee (*Apis mellifera*). A light and electron microscopical study. Neuroscience 38:797–807

Simon JC, Pfrender M, Tollrian R, Tagu D, Colbourne J (2010) Genomics of environementally-induced phenotypes in two extremely plastic arthropods. J Hered (in press)

Sokal RR, Rohlf FJ (1995) Biometry. Freeman, New York

Staudacher EM, Gebhardt M, Dürr V (2005) Antennal movements and mechanoreception: neurobiology of active tactile sensors. Adv Insect Physiol 32:49–205

Steel CG (1977) The neurosecretory system in the aphid *Megoura viciae*, with reference to unusual features associated with long distance transport of neurosecretion. Gen Comp Endocrinol 31:307–322

Steel CG, Lees AD (1977) The role of neurosecretion in the photoperiodic control of polymorphism in the aphid *Megoura viciae*. J Exp Biol 67:117–135

Stocker RF, Lienhard MC, Borst A, Fischbach KF (1990) Neuronal architecture of the antennal lobe in *D. melanogaster*. Cell Tissue Res 262:9–34

Strausfeld NJ (2005) The evolution of crustacean and insect optic lobes and the origins of chiasmata. Arthropod Struct Dev 34:235–256

Strausfeld NJ, Hansen L, Lie YS, Gomez RSS, Ito K (1998) Evolution, discovery, and interpretation of arthropod mushroom bodies. Learn Mem 5:11–37

Strausfeld NJ, Sinakevitch I, Brown SM, Farris SM (2009) Ground plan of the insect mushroom body: functional and evolutionary implications. J Comp Neurol 513:265–291

Strauss R (2002) The central complex and the genetic dissection of locomotor behavior. Curr Opin Neurobiol 12:633–638

Tagu D, Klingler JP, Moya A, Simon JC (2008) Early progress in aphid genomics and consequences for plant-aphid interactions studies. Mol Plant Microbe Interact 34:809–822

Tilley SB, Weaver RJ, Isaac RE (2000) Allatostatin-like and AKH/HrTH-like peptides in the aphid *Megoura viciae*. Gen Comp Endocrinol 117:355–365

Utz S, Huetteroth W, Voemel M, Schachtner J (2008) Mas–allatotropin in the developing antennal lobe of the sphinx moth *Manduca sexta*: distribution, time course, developmental regula-tion, and colocalization with other neuropeptides. Dev Neurobiol 68:123–142

Veenstra JA, Hagedorn HH (1993) Sensitive enzyme immunoassay for *Manduca* allatotropin and the existence of an allatotropin–immunoreactive peptide in *Periplaneta americana*. Arch Insect Biochem 23:99–109

Zhou J-J, Vieira FG, He X-L, Smadja C, Liu R, Rozas J, Field LM (2010) Genome annotation and comparative analyses of the odorant-binding proteins and chemosensory proteins in the pea aphid *Acyrthosiphon pisum*. Insect Mol Biol 19:113–122